

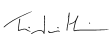
Calibrating MARSS By The Tip Curve Method

Tim Hewison
David Pollard

MRF Technical Note No. 42
Issue: 1
3 October 2002

(14 pages)

Controlled Copy Number: - N/A.

	Name	Date	Signature
Document Prepared by	Tim Hewison	3/10/02	
Document Checked by	Jonathan Taylor		
Document Authorised by	Jonathan Taylor		

This document replaces all previous issues

Met Office
Building Y70, Cody Technology Park
Ively Road, Farnborough
Hampshire GU14 0LX, UK

Tel: +44 (0)1252-395781
Fax: +44 (0)1252-370789
E-mail: tim.hewison@metoffice.com



1. Introduction

MARSS is a total power radiometer. It incorporates two on-board black body calibration targets which are maintained at contrasting temperatures to allow the gain and offset to be calculated. High gain is needed to amplify the signal from thermal levels to detectable power levels. This introduces instability in the system, which means the calibration must be conducted frequently and over the full range of conditions experienced in operation.

However, the calibration targets have several practical difficulties [McGrath & Hewison, 2001]. Most importantly, a thermal gradient is present across the thickness of the absorbent coating of the hot target, due to its poor thermal conductivity. Factors such as this can introduce a bias into the calibrated brightness temperatures. Until now, this bias has been evaluated by comparing the brightness temperatures measured when viewing scenes of "known" radiance - a liquid nitrogen target on the ground [Hewison & McGrath, 2001] or low zenith brightness temperatures in flight at high level. Such comparisons were used to derive corrections to the hot target temperature measured by Platinum Resistance Thermometers in its base. These hot target corrections were then parameterised in terms of an observable variable, such as target power, and applied to all operational data. Typically, these corrections increased the brightness temperatures by several kelvin at high level.

The underlying assumption behind this technique is that reference brightness temperatures can be accurately modelled. This assumption has been brought to question by recent analysis of the validation of atmospheric absorption models using MARSS data. Although the various models tend to agree that atmospheric absorption in the window channels is low in cold, dry conditions, that analysis suggests that all models underestimate the absorption by ~50%. This can amount to a difference of several kelvin in the reference brightness temperatures used to calibrate the radiometer. This, in turn, can introduce a bias when calculating absorption over finite layers for model validation. Thus this method cannot be relied upon for absolute calibration validation and other methods must be investigated.

Instrument	MARSS				
AMSU Channel	16	17	18	19	20
Frequency (GHz)	89	157	183±1	183±3	183±7
View Angles (along track)	Up and Down +40° to -40°				
Scan Period (s)	3				
Polarisation angle in zenith view	0°	40°	42°		
Beamwidth (FWHM)	11.8°	11.0°	6.2°		
Integration time (ms)	100				
Sensitivity NEΔT (K)	0.5	0.7	0.6	0.4	0.3
Cal. Accuracy (K)	0.9	1.1	1.0	0.9	0.8

Table 1 - Characteristics of MARSS

2. Tip Curve Calibration Outline

This report concentrates on the application of the 'Tip Curve' method of calibration. The underlying theory is that the down-welling radiance varies with zenith angle in a way that can be well modelled, allowing the observations to be adjusted until they obey this "rule".

In the case of an upward viewing microwave radiometer operating with channels in the "window" regions of the spectrum, the radiative transfer equation can be approximated to :

$$T_Z(\theta) = T_{MR} \cdot (1 - e^{-\tau \cdot \sec(\theta)}) + T_{CMB} \cdot e^{-\tau \cdot \sec(\theta)} \quad (1)$$

where $T_Z(\theta)$ is the brightness temperature at zenith angle, θ ; T_{MR} is the mean radiative temperature of the atmosphere; τ is the zenith opacity of the channel in question; T_{CMB} is the effective brightness temperature of the Cosmic Microwave Background consistent with the definition of Rayleigh Jeans equivalent brightness temperature [Janssen, 1993], which is linear with radiance, $T_{CMB} = (h \cdot \nu / 2 \cdot k) = 3.27$ K at 89 GHz, 4.28 K at 157 GHz and 4.77 K at 183 GHz.

The assumptions inherent in (1) are that the atmosphere is horizontally stratified, which essentially requires clear skies, as cloud is rarely homogeneous, and optically thin.

3. Tip Curve Calibration in Practice

The starting point for the tip curve calibration procedure are down-welling brightness temperatures, $T_Z'(\theta)$ measured over a range of zenith angles, θ , calculated from the radiometer's system equation. (These values may already include a hot target correction, based on previous calibrations calculated with respect to modelled radiances at high level.)

In practice, the tip curve is used to retrieve a best estimate for the true zenith brightness temperature, T_{ZO} . The calibration is then revised so the corrected measurements are consistent with this value. This is an iterative process, which is repeated until the results converge.

The first step is to produce an initial estimate of the opacity, τ , in each view:

$$\tau(\theta) = \ln \left(\frac{T_{MR} - T_{CMB}}{T_{MR} - T_Z'(\theta)} \right) \quad (2)$$

Calculating the Atmospheric Mean Radiative Temperature

For optically thin cases, T_{MR} can be estimated as an average of the vertical temperature profile, T_i , weighted by the humidity mass mixing ratio, q_i , assuming most of the absorption is due to water vapour.

$$T_{MR} = \frac{\sum_i T_i \cdot q_i}{\sum_i q_i} \quad (3)$$

This has been calculated for several profiles, and found to be linearly related to the air temperature at any level in the troposphere, T_{air} with an rms error of 1.8 K as follows:

$$T_{MR} = 16.35 + 0.9018 \cdot T_{air} \quad (4)$$

For a typical mid-latitude flight (A808), the air temperature was found to be related to MARSS cold target temperature, T_c with an rms error of 0.8 K as follows:

$$T_{air} = 1.133 \cdot T_c - 45.1 \quad (5)$$

Thus for flight data, T_{MR} can be estimated in terms of MARSS' cold target temperature, a variable that is readily available in the datasets, with an rms uncertainty of 2.25 K. However, this technique is not valid for use on the ground as solar heating can increase the cold target temperature to the extent that (5) would introduce a bias. In these cases, the zenith brightness temperature measured by MARSS' Ch20 can be used as a proxy for T_{MR} as this was found to be close to the value calculated by (3) for the CLIWA-NET experiment. However, this will not generally be true for all conditions.

Finite Beamwidth Correction

MARSS' field of view integrates a finite region of the sky, which in general will have a brightness temperature gradient with zenith angle. The initial estimate of τ is needed to apply a correction for the finite beamwidth of MARSS' channels [Han & Westwater, 2000]. Equation (6) describes the increase in apparent brightness temperatures, dT_z , caused by this.

$$dT_z(\theta) = \frac{FWHM^2}{16 \cdot \ln(2)} \cdot (T_{MR} - T_{CMB}) \cdot e^{-\tau(\theta)} \cdot \left[(2 + (2 - \tau(\theta)) \cdot \tan(\pi/2 - \theta))^{-2} \right] \cdot \tau(\theta) \quad (6)$$

where FWHM is the Full Width Half Maximum power beamwidth of the channel, given in Table 1.

Fitting the Tip Curve

Figure 1 shows typical brightness temperatures measured by MARSS' 89 GHz channel on ground during CLIWA-NET. For the experiment, MARSS' pod was rotated by 40° to increase the range of zenith angles observed.

Error! Reference source not found. shows the calculated opacity, $\tau(\theta)$, with airmass, $sec(\theta)$, again for a period of clear skies on the CLIWA-NET experiment (02/08/02 1130-1200 UTC). It can be seen that at higher zenith angles, the atmosphere becomes optically thick, and the relationship between opacity and airmass becomes non-linear. This occurs at lower zenith angles for the 157 GHz channel. At high zenith angles, the Earth's curvature also becomes a significant factor [Han & Westwater, 2000], and the correction for finite beamwidth (6) becomes critical.

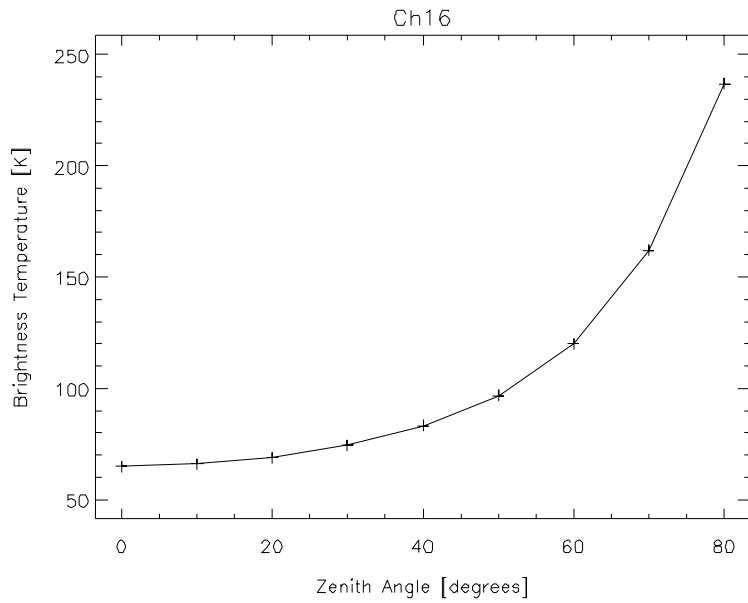


Figure 1 - Brightness temperatures measured by MARSS' 89 GHz channel

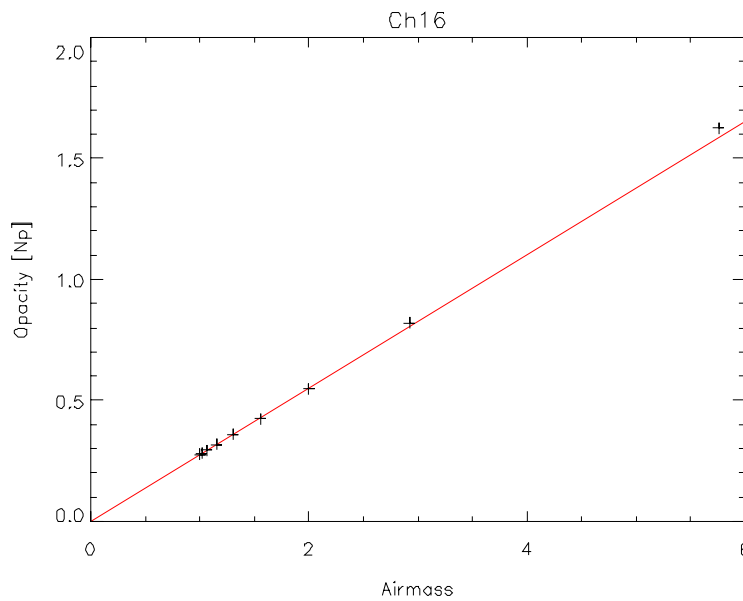


Figure 2 - Measured (+) and fitted (—) variation of Opacity, (τ), with Airmass, $\sec(\theta)$

Theoretically, the opacity would be zero for a hypothetical airmass of zero. This fact is exploited to reduce the number of degrees of freedom when fitting the tip curve. Those observations with zenith angle, $\theta < 50^\circ$ are used to estimate the mean slope, $\langle \tau / \sec(\theta) \rangle$, which is also equivalent to the best estimate of the opacity at zenith and consequently the brightness temperature, T_{z0} .

The observed brightness temperatures are then corrected to be consistent with the tip curve and the whole tip curve process is iterated until the results converge. This can be done in many ways, two of which are described here.

Deriving a hot target correction

The radiometer's system equation can be modified to include a correction to the hot target temperature, δT_h . This can be evaluated using the slope fitted to the tip curve thus:

$$dT_h = \left[T_{MR} \cdot (1 - e^{-\langle \tau / \sec(\theta) \rangle \cdot \sec(\theta_0)}) + T_{CMB} \cdot e^{-\langle \tau / \sec(\theta) \rangle \cdot \sec(\theta_0)} - T_Z(\theta_0) \right] \cdot \frac{(T_h - T_c)}{(T_Z(\theta_0) - T_c)} \quad (7)$$

where θ_0 is the zenith angle at the nominal zenith view (or any other) and T_h and T_c are the hot and cold target temperatures, respectively.

Deriving a non-linearity correction

Analysis of tip curve calibrations suggests a different correction is necessary for Ch16 than MARSS' other channels. This has previously been explained by the different penetration depth of the lower frequencies into the microwave absorber coating on the target or greater sensitivity of this channel to thermal gradients across the target, due to its broader quasi-optical beamwidth. However, the results of the tip curve calibration suggest another mechanism may be influencing Ch16.

The IF power level at the detector of MARSS' Ch16 has always been higher than recommended by RAL. This could result in a non-linearity in the detector, although it has previously been difficult to detect this. Unfortunately, this channel was effected by Radio Frequency Interference during the instrument's characterisation in the vacuum facility [McGrath & Hewison, 2001]. Such a non-linearity would cause the radiometer's system equation to underestimate low brightness temperatures, T_z , when extrapolating from the warmer reference calibration targets. This bias, dT_z can be modelled by the arbitrary function:

$$dT_z = \gamma \cdot (T_h - T_z) \cdot (T_c - T_z) \quad (8)$$

where γ is the non-linearity factor.

This non-linear correction should be applied in addition to the thermal gradient correction, which is then assumed to be constant for all channels.

4. Application of Tip Curve to Flight Data

During high level flight, zenith brightness temperatures are expected to be low in all of MARSS' channels. Atmospheric temperatures are also low, increasing the thermal gradient through the hot target's absorber coating. The tip curve allows evaluation of the effect of hot target thermal gradient and/or receiver linearity for all channels at the limit of the operating envelope.

Prior to flight A777, Ch16 experienced RFI due to Local Oscillator leakage from the 183 GHz channels. This was then rectified by modifying the Ch 16 bandpass filters to match the equivalent channel of AMSU-B. Since flight A822, MARSS' control software was modified to supply a constant power level to the hot target (subject to a user-defined maximum operating temperature). This produces more stable thermal gradients, so I will take an example flight after this change: A830, which was MARSS' last science flight on the C-130. The period of 1129-1138 was during a run under thin Cirrus, which is not expected to

influence these channels significantly. This run is typical of others previously used in the evaluation of the hot target correction, which generally produce consistent results.

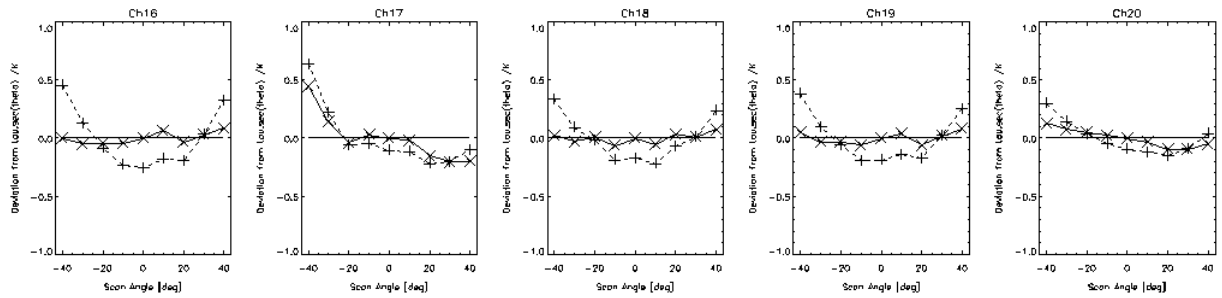


Figure 3 - Residuals from Tip Curve before (---+---) and after (—x—) correction for high level run at FL240 on flight A830 1129-1138

Figure 3 shows the deviations of the brightness temperatures from the theoretical variation of τ with $\sec(\theta)$ before and after corrections calculated from the tip curve have been applied. The tip curve calibration process reduces the residuals, although there is some residual view dependence, which is discussed below.

Table 2 shows the calculation of a revised form of hot target and non-linearity correction. The data in this table is taken from 10 high level runs during POLEX [Selbach *et al.*, 2002] (transits have been omitted). These runs were previously used to establish a hot target correction, with standard deviations of ~ 0.25 K, which is listed in the 2nd row of Table 2. This is based on the measured heater power, P , multiplied by a *Power Gradient* factor, dT_h/dP .

Table 2 also shows the increment to the hot target correction derived from the average of tip curves applied to the same high level runs. These have a standard deviation of ~ 0.1 K during runs, but were found to produce results that depended strongly on the airspeed, which was not obvious in the previously calculated hot target corrections.

The *Power Gradient* derived from the tip curve for the higher frequency channels is broadly consistent, but Ch16 requires a value almost twice as high to fit the tip curve. This is believed to be unphysical, so it is proposed that a common value of 0.085K/W is adopted for all channels. A non-linearity correction of the form expressed in Equation (8) is then introduced to explain the behaviour of Ch16.

Table 2 - Results of Tip Curve from all High Level runs since A822

MARSS Channel	Ch	16	17	18	19	20	
Hot Target Power	P	20	20	20	20	20	W
Previous Hot Target Correction	dT_h'	2.27	1.09	0.70	1.47	1.32	K
Previous Power Gradient	dT_h/dP	0.115	0.060	0.060	0.060	0.060	K/W
Tip Curve Increment to dT_h	ΔdT_h	1.09	0.41	0.68	0.72	0.38	K
Total Hot Target Correction	dT_h	3.35	1.49	1.38	2.19	1.70	K
Tip Curve Power Gradient	dT_h/dP	0.168	0.075	0.069	0.110	0.851	K/W
Proposed Power Gradient	dT_h/dP	0.085\pm0.009					K/W
Proposed non-linearity factor	γ	66x10⁻⁶	0	0	0	0	K ⁻¹

5. Application of Tip Curve to Ground Data

During low level flight or ground based operation, higher temperatures and opacities are expected. This allows the thermal gradients and/or receiver linearity to be evaluated at the other extreme of the operating envelope.

During August 2001, MARSS was operated on the ground for the Microwave Radiometer Intercomparison Campaign (MICAM) part of the CLIWA-NET experiment. The pod was rotated by 40° , so it scanned $\theta = 0 - 80^\circ$. The skies were mostly clear for the first 2 days of August, but cloudy later. The period 1130-1200 on 2/8/01 is used here., although almost identical results were obtained for 1550-1600 on 1/8/01.

The atmosphere is generally optically thick in the 183 GHz channels, and the tip curve method cannot be employed. In this case, at 157 GHz $\tau \sim 1$ at zenith, and higher zenith angles are seen to deviate significantly from the expected values, which suggests the tip curve may be invalid here too.

Figure 4 shows the deviation of the brightness temperature from the theoretical form of $\tau \cdot \sec(\theta)$ before and after corrections were applied to fit the tip curve. This process dramatically reduced the residuals for Ch16 from $\theta=0-50^\circ$, but left large excesses at higher zenith angles. These results were consistently observed throughout the experiment. At 157 GHz, this trend is present in the residuals for all angles, which suggests it is a systematic bias introduced by the Equation (1) breaking down for high opacities ($\tau > 1$).

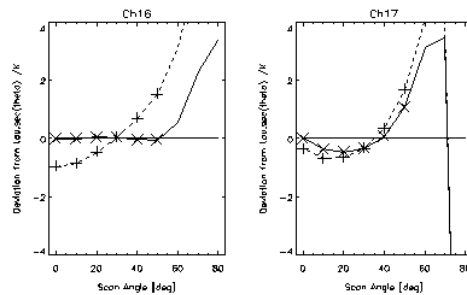


Figure 4- Residuals from Tip Curve before (---+---) and after (—x—) correction for Ground-based use in CLIWA-NET MICAM 02/08/01 1130-1200 UTC $0^\circ \leq \theta \leq 50^\circ$ only Symbols show views included in Tip Curve calculation. Lines show all points.

Part of the original motivation to investigate tip curve calibration was an attempt to resolve the difference between the observations of MARSS' 89 GHz channel and the 90 GHz channel of MICCY during MICAM. The data issued for MARSS based on hot target corrections derived prior to this study were consistently ~ 5 K higher than the equivalent MICCY data. As MICCY's calibration is partially based on tip curves, it was thought this technique may be introducing a bias. However, these results show that applying the tip curve to MARSS data during MICAM, systematically increases the zenith brightness temperatures, further increasing the difference with MICCY. This may be partially explained if MICCY's tip curve includes the higher zenith angles, which were found to have systematically positive residuals from the tip curve. This is thought to be caused by a large scale humidity gradient present during the period of this calculation. It is, therefore recommended that the MICCY calibration be re-examined to check for similar features.

6. Application of Aircraft Data in Profiles

The relative calibration of MARSS in profiles is of critical importance in the validation of absorption models. To test MARSS performance with respect to the tip curve calibration, flight A808 was analysed. This flight included a transit at mid-level, a profile down, a spiral ascent, runs and a transit at high-level before the final descent.

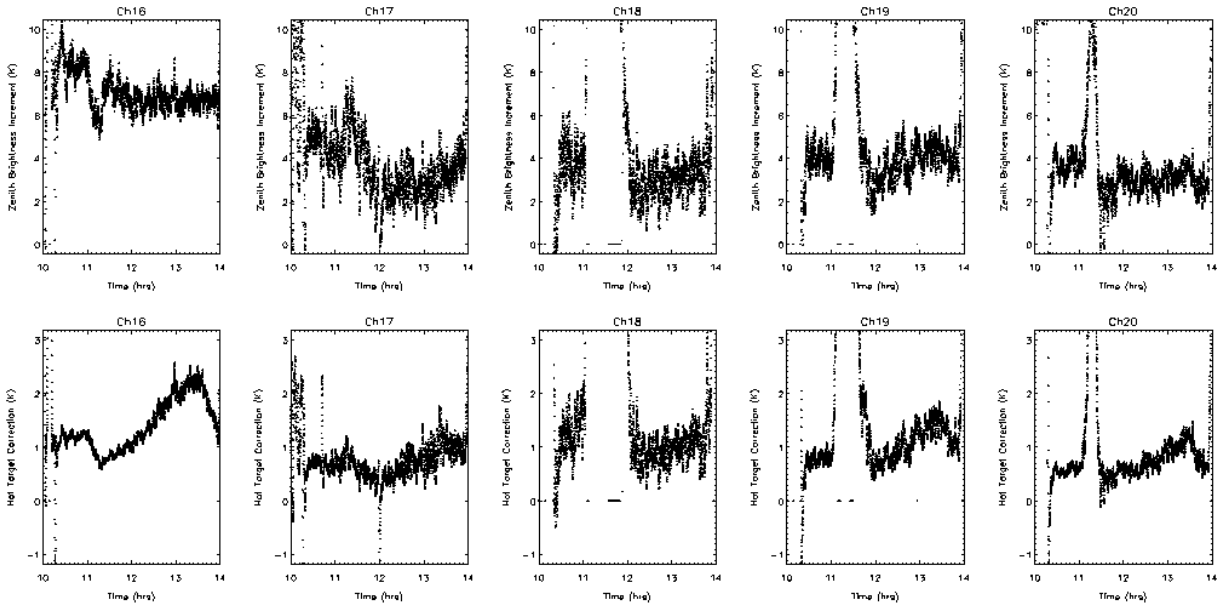


Figure 5 - Time Series of Brightness Temperature Increments from Tip Curve for flight A808

Figure 5 shows time series of the correction applied to zenith brightness temperatures by the tip curve for all the MARSS channels over flight A808. The data plotted here have *not* already had a hot target correction applied. On this flight, the hot target was maintained at a constant temperature (312 K). This requires increasing the power to the target heater during the spiral ascent, which results in the steady increase in the hot target correction during the period 11:22:55 – 13:19:50. During the period prior to this, the tip curve produces consistent results for the higher frequency channels (17–20).

However, the tip curve produces significantly different results for Ch16, suggesting this channel is sensitive to another process related to the thermal environment (and not just the receiver non-linearity). These results are very difficult to model in terms of any other observable parameter. It is therefore recommended that if Ch16 data is to be used in profiles, the tip curve calibration is applied dynamically to correct the data for this poorly understood mechanism. This may be implemented by constructing a time series of brightness temperature correction. This can then be smoothed to reduce the noise, assuming the mechanism responsible for the bias varies only slowly.

7. Error Analysis

Errors can be introduced at any stage in the process of performing and analysing tip curve calibrations. Random errors will tend to be reduced by integrating radiometer data over time. Systematic errors are reviewed in this section by perturbing each parameter by an estimate of its uncertainty and repeating the tip curve calculation. These calculations were repeated for different operating conditions: High level flight and Ground-based operation, with the pod inclined to scan from zenith to $\theta=80^\circ$. The results are presented in Table 3 and Table 4.

Table 3 - Sensitivity of Fitted Zenith Brightness Temperature to each term of Tip Curve for High Level run during Flight A830 1129-1138 FL240

Channel	16	17	18	19	20	
Previous T_z	6.96	6.66	24.35	9.76	7.32	K
Corrected T_z	9.51	7.73	25.98	11.61	8.27	K
$T_{MR}-2.25K$	0.00	0.00	0.02	0.00	0.00	K
$T_{MR}+2.25K$	0.00	0.00	-0.01	-0.01	0.00	K
$\theta-0.5^\circ$	0.15	0.09	0.50	0.17	0.09	K
$\theta+0.5^\circ$	-0.15	-0.08	-0.48	-0.17	-0.09	K
$FWHM-50\%$	-0.10	-0.05	-0.08	-0.03	-0.02	K
$FWHM+50\%$	0.17	0.09	0.14	0.05	0.02	K
$\sigma-50\%$	-0.94	-0.23	-0.16	-0.17	-0.17	K
$\sigma+50\%$	0.37	0.14	0.11	0.08	0.09	K
$pol-5^\circ$	0.00	-0.46	-0.48	-0.51	-0.52	K
$pol+5^\circ$	-0.06	0.55	0.56	0.57	0.57	K
Total uncertainty	0.75	0.55	0.73	0.58	0.57	K

Table 4 - Sensitivity of Fitted Zenith Brightness Temperature to each term of Tip Curve for Ground-based use in CLIWA-NET MICAM 02/08/01 1130-1200 UTC $0^\circ \leq \theta \leq 50^\circ$ only

Channel	16	17	
Previous T_z	64.9	156.5	K
Corrected T_z	70.7	158.3	K
$\tau < 0.5$	0.00	N/A	K
$\tau < 1.0$	1.22	-1.68	K
$\tau < 1.5$	1.22	0.00	K
$T_{MR}-2.25K$	0.09	0.75	K
$T_{MR}+2.25K$	-0.09	-0.68	K
$\theta-0.5^\circ$	2.00	3.72	K
$\theta+0.5^\circ$	-1.83	-3.49	K
$FWHM-50\%$	0.01	0.01	K
$FWHM+50\%$	-0.05	-0.09	K
$\sigma-50\%$	0.35	0.62	K
$\sigma+50\%$	-0.17	-0.25	K
$pol-5^\circ$	-0.29	0.07	K
$pol+5^\circ$	0.29	-0.11	K
Total uncertainty	2.31	4.07	K

High Opacity

The underlying assumption in the tip curve calibration is that the atmosphere is optically thin and can be represented by a Mean Radiative Temperature, T_{MR} . Although "optically thin" is usually taken to mean $\tau < 1$, the transition is not strictly defined, but represents a gradual introduction of bias. For the purposes of this analysis, only views with $\tau < 1$ are included. The sensitivity to this threshold is investigated by comparing the results with those obtained using thresholds of $\tau < 0.5$ and $\tau < 1.5$.

The selection of this threshold is not relevant to the high-level run, as $\tau \ll 1$ for all channels.

For ground-based use, the selection of this threshold has a significant impact on both Channels 16 and 17. This threshold selects which views are included in the tip curve calculation, and higher zenith angles are systematically higher than expected for both channels. For this reason, only zenith angles $0^\circ \leq \theta \leq 50^\circ$ are included in the calculation. The reason for the large residuals in the tip curve calculation for 89 GHz at $\theta = 60^\circ$ is uncertain. It may be due to systematic humidity gradient, associated with this coastal area (see below).

Mean Radiative Temperature

In normal flight conditions, equations (4) and (5) are believed to estimate T_{MR} with an rms uncertainty of 2.25 K. To investigate the sensitivity of the tip curve results to T_{MR} the calculation was repeated after perturbing T_{MR} by ± 2.25 K. This was found to have a negligible impact for views with low opacity, but significant for Ground-based operation at 157 GHz. The tip curve becomes critically sensitive to T_{MR} when $\tau > 1.5$.

Zenith Angle Misalignment

Any misalignment of the MARSS pod will introduce a systematic offset in the zenith angle of all views, which will bias the tip curve calculation. To test the sensitivity to this term, the zenith angle was perturbed by $\pm 0.5^\circ$ and the tip curve calculation repeated. This is an estimate for the repeatability of the installation both on the aircraft and in ground-based operation during CLIWA-NET. The results show even these small offsets introduce significant bias in the retrieved zenith brightness temperature, although this is reduced when using views on both sides of zeniths. This term dominates the error budget when $\tau > 0.1$. In future it is recommended that the pod angle is carefully measured at the time of installation, during and after experiments, and that the pod is approximately horizontal. This will produce a more symmetric distribution of angles around zenith, reducing the impact of any misalignment.

Mirror Reflectivity

As MARSS' mirror rotates, the polarisation angle incident upon it also rotates. As the reflectivity of the mirror changes with polarisation angle, this introduces a view dependent bias of ~ 1 K. This is described in more detail in [McGrath & Hewison, 2001]. This bias is routinely corrected for as part of the MARSS processing, but there remains a residual view dependence due to the uncertainty in the terms representing the mirror conductivity, σ ($\pm 50\%$), and the polarisation angle incident, pol ($\pm 5^\circ$). These terms are the dominate source of uncertainty when applying the tip curve to high level flight data from channels with low opacity. In the case of Ch16 the conductivity term dominates, while at higher frequencies, the polarisation angle dominates, due to their different orientation.

Finite Beamwidth Correction

Although the beamwidth is known to better than $\pm 2^\circ$, there is still the possibility of contamination by sidelobes exposed to scenes of contrasting brightness. This is represented by repeating the tip curve calculation by perturbing the $FWHM$ term in (6) by $\pm 50\%$. This was found to have a minimal impact for the range of zenith angles used, but becomes significant at higher angles.

Solar Contamination

If the sun is within twice the beamwidth of a channel's beam centre, it is likely that the view will be contaminated to some extent. Some cases are easy to identify by inspection, where there is a deviation of ~10K in the brightness temperature. More accurately, the angle between the Sun and MARSS' field of view can be calculated, as described by [Jones, 1995]. Otherwise, there remains the possibility that undetected solar contamination will bias the tip curve.

In examination of the residuals for the high level tip curve, there appears to be a small bias in *Scan Angle*=-40° view. This maybe due to contamination of this view by the aircraft's wing, although the leading edge of which subtends an angle of ~64° to the pod, so it should be well clear. However when this view is omitted the tip curve produces very different results, retrieving a much higher zenith brightness and producing much stronger view dependence in the residuals. The reason for this is not clear at present.

Horizontal Homogeneity

One of the underlying assumptions in the tip curve method is that the atmosphere is horizontally stratified. This implies it should be cloud free, which is easy to detect. For ground-based operation, atmospheric variability introduces more variability between consecutive scans (3s) than the radiometer's random noise. In flight at high level the opposite is true. Any random fluctuations in humidity associated with turbulence or convection will be averaged if left to advect across range of zenith angles. This will happen rapidly in flight at high level, but may take several minutes on the ground.

Overall, it was found that the tip curve produced lowest random errors at zenith brightness temperatures $T_z \sim 60$ K, but lowest systematic errors for $10 \text{ K} < T_z < 30 \text{ K}$.

However, systematic humidity gradients associated with coastal areas or frontal passages will not be averaged out in this way, and will introduce a systematic bias in the tip curve, which may be visible in the residuals. This may explain some of the large residuals observed at high zenith angles during CLIWA-NET, when the Total Water Vapour was observed to increase at a rate of ~5%/hr on 2/8/01 as a front approached from the West. It would be easier to quantify this effect with full azimuthal scans, or with views not arranged symmetrically around zenith.

It is, therefore, recommended that in future, the tip curve is only applied when the zenith brightness temperature changes sufficiently slowly over an extended period to minimise view dependent biases.

Earth's Curvature

A detailed analysis shows the Earth's curvature has negligible impact on the tip curve calculation for zenith angles, $\theta < 60^\circ$ [Han & Westwater, 2000].

8. Summary of Results and Recommendations

The tip curve has been investigated as a possible technique to provide MARSS with a calibration reference point for a range of operating conditions. Previously the calibration has relied on an unbiased radiative transfer model to provide a reference brightness temperature close to the cosmic microwave background at high level, where there was very little absorbing material above the aircraft. However, these models have recently been found to have large biases in these conditions, so an alternative technique must be sought.

The tip curve was found to provide a useful calibration reference in the following conditions:

- Optically thin ($\tau < 1$) This is generally true at 89 GHz, and often at 157 GHz, but only applies to the 183 GHz channels at higher altitudes.
- Homogeneous This implies the sky must be completely free of any cloud over the angular range and duration of the calibration.
- Low zenith angle Not a problem for MARSS in its normal configuration, but systematic biases were observed at $\theta > 50^\circ$.
- Zenith angle known Uncertainties in the zenith angle of $> 0.5^\circ$ introduce large biases.

The rms accuracy of the tip curve approaches 0.5 K at high level ($T_z \sim 10$ K), where uncertainty in the view dependence dominates. At low level, the uncertainty increases with zenith brightness, due to the limited pointing accuracy. For $T_z = 70$ K, the rms accuracy is ~ 2 K.

The tip curve technique was applied to a series of high level runs. It was found that, in order to match the derived zenith brightness, a correction of $dT_h = (0.085 \pm 0.009) * P$ should be applied to the hot target temperature measured in its base, where P is the heater power. This is larger than the value previously applied, derived from radiative transfer calculations. A residual bias was observed in Ch16, which is thought to be due to the high IF signal level input to the detector in this channel. This bias should be removed by applying a non-linearity correction.

However, when applying the tip curve to flight data in profile descents, where the thermal environment is changing rapidly, substantial biases are observed, especially in Ch16. As these biases are not easily modelled in terms of any observable variable, it is recommended that the tip curve calibration be applied dynamically to correct these data.

The tip curve did not help reduce the systematic differences between the measurements of MARSS and MICCY at 89 and 90 GHz respectively. In fact, applying the tip curve calibration to MARSS increased this difference! This may be partially explained if MICCY's tip curve calibration is being biased by systematically higher brightness temperatures at higher zenith angles, as observed by MARSS. It is recommended that in future, the tip curve is only applied when the zenith brightness temperature changes sufficiently slowly over an extended period to minimise view dependent biases.

9. References

S.Crewell, 2001: "MICAM: Microwave Radiometer Intercomparison Campaign" Website, <http://r203d.meteo.uni-bonn.de/CLIWANET/MICAM/> (User: MICAM passwd: cabauw@nl)

C.Gaffard, 2001: "Cabauw field experiment 01-08-2001/14-08-2001 Descriptive Report" Unpublished report.

Y.Han and E.R.Westwater, 2000: "Analysis and Improvement of Tipping Calibration for Ground-Based microwave radiometers," IEEE-TGARS, Vol.38, No.3, 2000, pp.1260-1276.

T.J.Hewison and A.J.McGrath 2001: "Performance assessment of Liquid Nitrogen Calibration Target supplied by Fred Solheim (Radiometrics) at 89, 157 and 183 GHz," MRF Technical Note 39, 2001.

M.A.Janssen, 1993: "Atmospheric remote sensing by microwave radiometry," Wiley Series in Remote Sensing, Chapter 1.

D.C.Jones, 1995: "Validation of scattering microwave radiative transfer models using an aircraft radiometer and ground-based radar," PhD Thesis, University of Reading, Dept. of Meteorology.

A.J.McGrath and T.J.Hewison, 2001: "Measuring the accuracy of a Microwave Airborne Radiometer (MARSS)", Journal of Atmospheric and Oceanographic Tech., Vol.18, No.12, 2001, pp.2003-2012.

N.Selbach, T.Hewison, G.Heygster, J.Miao, A.McGrath, J.Taylor 2002: "Validation of total water vapor retrieval with an airborne millimeter-wave airborne radiometer over Arctic sea ice", Accepted for publication in Radio Science, 2002.